Approach for ambipolar behaviour suppression in tunnel FET by workfunction engineering

Kaushal Nigam ✉, *Pravin kondekar, Dheeraj Sharma*

Electronics and Communication Engineering Discipline, Indian Institute of Information Technology, Jabalpur 482005, India
✉ *E-mail: connecttokaushal@gmail.com*

Published in Micro & Nano Letters; Received on 19th April 2016; Accepted on 23rd May 2016

A dual material control gate tunnel field effect transistor (TFET) for asymmetric doping at source and drain regions is proposed. The gate consists of three segment different workfunctions ϕ_1, ϕ_2, and ϕ_3, which are named as tunnelling gate (M_1), control gate (M_2), and auxiliary gate (M_3), respectively. Forward to this, three possible combinations of ϕ_1, ϕ_2 and ϕ_3 to maintain the dual workfunctionality of the device ($\phi_2 = \phi_3 > \phi_1$, $\phi_1 = \phi_2 > \phi_3$, $\phi_1 = \phi_3 < \phi_2$) were considered. Further, the comparison of these possible combinations are performed with conventional TFET ($\phi_1 = \phi_2 = \phi_3$). Among these $\phi_1 = \phi_3 < \phi_2$, generates most optimum results in terms of suppression of ambipolar behaviour, and enhancement in ON state current (I_{ON}) of the device. The proposed device shows significant improvement in terms of I_{ON} (1.66×10^{-5} A/μm for SiO_2), I_{ON}/I_{OFF} (7.22×10^{11}), and sub-threshold swing (~19 mV/decade) as compared with conventional and the dual material TFET devices. Further, the analysis of analogue/RF performance is performed for the devices showing optimum performance in terms of suppression of ambipolar behaviour.

1. Introduction: The scaling of MOSFET is creating several problem such as short channel effects, hot carrier effects (HCEs), subthreshold leakage current, static power dissipation and subthreshold slope physical limits to 60 mV/decade at room temperature. Hence, the replacement of MOSFET become necessary. In this regards, tunnel field effect transistor (TFET) is a promising candidate to overcome these issues by using quantum tunnelling mechanism, which is based on the band to band tunnelling of carriers [1–5]. Whereas, TFET has its own limitations such as inferior ON-state current and the ambipolar behaviour which degrades the performance of the device. According to International Technological Road-map for semiconductor requirements [6], the ON-state current and ambipolar behaviour of TFET are the major problem of the device. For this, various approaches (strain silicon, pocket doping, hetero gate dielectric, etc.) have been proposed earlier to improve the ON-state current [7–15]. However, the ambipolar behaviour of TFET is due to the presence of symmetric n^+ and p^+ regions. Therefore, it shows n-type tunnelling with positive gate voltage and p-type tunnelling with negative gate voltage in case of n-TFET and vice versa for p-TFET. Thus, similar transfer characteristics in case of positive and negative gate bias, leads to parasitics conduction at OFF-state condition. To overcome the problem of ambipolar behaviour, various methods have been used in TFET such as (i) using heterogeneous gate dielectric (ii) using various doping profile in the drain region (iii) using large band gap material on the drain side to increase the tunnelling width [16, 17]. Although the above mentioned method reduces the ambipolar conduction, they can lead to (i) reduction in ON-state current, (ii) increases the drain series resistance and (iii) added process complexity. Hence, the improvement in I_{ON} and suppression in ambipolar behaviour of the device are issues of grave concern. In order to overcome these problems, we investigate a novel approach dual material control gate TFET (DMCG-TFET) with asymmetric doping in source and drain regions. For this, the different values of workfunction for tri-segmented DMCG-TFET are considered to maintain dual work functionality of the device for suppression of ambipolar behaviour, HCEs and to enhance the ON-state current. The presence of lower workfunction at auxiliary gate relative to control gate reduces the band bending and lateral electric field strength at drain/channel junction by applying negative gate voltage which suppresses the ambipolar behaviour. However, the presence of lower workfunction at tunnel gate relative to control gate, increases the band bending and tunnelling probability at source/channel junction in the ON-State results in enhanced value of the ON current (I_{ON}). Further, the effect of dielectric material and temperature variation are considered of the proposed device to optimise I_{ON}/I_{OFF} ratio. Finally, the suppression of ambipolar behaviour is considered as a measure for selection of devices for the analysis of high frequency performance. However, the physical realisation of dual workfunction for gate electrode is a challenging task. The advancement in nanolithography and taking molybdenum as a gate material offer integration of dual work functionality [18, 19], using high dose nitrogen implantation.

The rest of the Letter is arranged as follows: Section 2 describe the device schematic, design specification and simulation setup. Whereas, Section 3 addresses the results and discussion. Section 4 demonstrates the analogue/RF performances. Finally, Section 5 summarises the important finding followed by conclusion.

2. Device schematic, design specification and design simulation setup: Figs. 1*a* and *b* illustrates the cross-sectional view of the conventional dual material gate-TFET (DMG-TFET) and proposed DMCG-TFET. The design parameters used in simulation of the proposed device are shown in Table 1. In proposed device, the gate comprises of three segments denoted by M_1, M_2 and M_3, respectively, as shown in Fig. 1*b*. The workfunction of control gate is 4.6 eV which is corresponding to molybdenum (Mo) (4.36 eV to 4.95 eV). However, the workfunction for tunnel and auxiliary gate are 4.0 eV which is corresponding to aluminium (Al) (4.0 to 4.26 eV). The technological computer aided design simulation has been performed by using 2D ATLAS. For this the non-local band to band tunnelling model is considered which uses Wentzel–Kramer–Brillouin approach for measuring the tunnelling probability through-out the tunnelling path. Shockley–Read–Hall and auger recombination are enabled for minority recombination effects. The band gap narrowing model is activated due to heavily doped concentration in the source and drain. In addition, the effect of quantum confinement and interface trap on band to band tunnelling in tunnel FET are accounted by using quantum confinement model.

© The Institution of Engineering and Technology 2016

doi: 10.1049/mnl.2016.0178

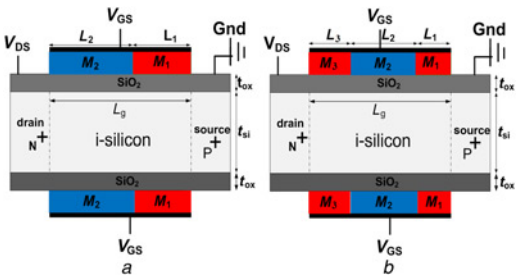


Fig. 1 *Schematic view of*
a Conventional dual gate material TFET
b Proposed DMCG-TFET

Table 1 Design parameters used in simulation of the device

Parameter name	Symbol	Value	Unit
channel length	L_{ch}	50	nm
gate oxide thickness	T_{ox}	1	nm
silicon film thickness	T_{si}	10	nm
channel doping	N_{ch}	1×10^{17}	cm^{-3}
source doping (*p*-type)	N_s	1×10^{20}	cm^{-3}
drain doping (*n*-type)	N_d	5×10^{18}	cm^{-3}
tunnelling gate length	L_1	10	nm
control gate length	L_2	25	nm
auxiliary gate length	L_3	15	nm
tunnel gate workFunction	ϕ_1	4.0	eV
control gate workfunction	ϕ_2	4.6	eV
auxiliary gate workfunction	ϕ_3	4.0	eV

3. Result and discussion: This section elaborates the performance of DMCG-TFET in terms of energy band diagram, transfer characteristics, output characteristics, comparison with other TFETs, and effect of dielectric and temperature variation on DMCG-TFET. Finally, comparison of analogue/RF performance is performed for DMCG TFET and DMG TFET2.

3.1. Energy band diagram of DMCG-TFET: From Figs. 2*a* and *b*, we can observe the effect of variation in workfunction of control gate (ϕ_2), keeping the fixed value of workfunction for tunnelling gate (ϕ_1) and auxiliary gate (ϕ_3), in OFF-state condition ($V_{GS} = 0$ V, $V_{DS} = 1$ V) and ON-state condition ($V_{GS} = 1.0$ V, $V_{DS} = 1.0$ V) of the device DMCG-TFET. Fig. 2*a* depicts the band diagram of OFF-state condition, from which we can note that, on increasing workfunction for control gate (ϕ_2), tunnelling width increases and band overlap on the source side decreases, which leads to reduction in OFF-state tunnelling probability. Whereas, for higher value of workfunction for control gate ($\phi_2 >$ 4.6 eV) band overlapping even appears in the drain region. Further, it can be observed that for smaller energy barrier width at drain/channel interface for $\phi_2 = 4.8$ eV, tunnelling occurs in OFF-state condition. While, in the ON-state condition, variation in workfunction of control gate brings only minute differences in the band diagram till specific value of workfunction is achieved ($\phi_2 = 4.6$ eV) as shown in Fig. 2*b*. However, for greater values of $\phi_2 (> 4.6$ eV), reduction in band overlapping have been spotted, over the section where the tunnel width is large.

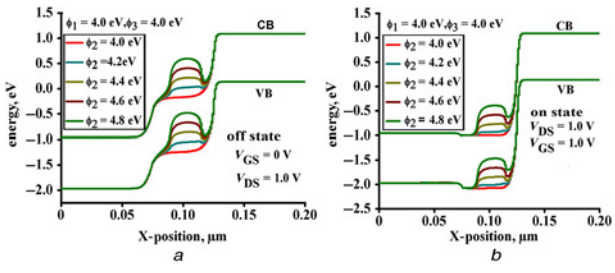


Fig. 2 *Energy band diagram along the channel direction in*
a OFF-State condition
b ON-State condition

3.2. Transfer and output characteristics of DMCG-TFET: Fig. 3 shows the transfer characteristics of the DMCG-TFET. The workfunction control gate (ϕ_2) has been increased from 4.0 to 4.8 eV, while keeping the fixed value of workfunction for tunnelling gate (ϕ_1) and auxiliary gate (ϕ_3). From the transfer characteristics, for various values of ϕ_2, it has been noted that leakage current (I_{OFF}) decreases till $\phi_2 = 4.6$ eV, due to decrement in band overlapping over the source region as shown in Fig. 2*a* and wider tunnelling width. In contrast to this, leakage current (I_{OFF}) increases on further increment in $\phi_2 (> 4.6$ eV), due to appearance of band overlapping over the drain region and tunnelling width barrier on drain side getting smaller. However, no significant change in ON-state current has been detected as shown in Table 2.

Fig. 4 demonstrates the output characteristics of DMCG-TFET for exponential and saturation region. From the same figure, it can be detected that there is no outstanding change in tunnelling width with V_{DS} under saturation region, hence, the current remains same in this region. Further, it can be spotted that drain current increases with gate to source voltage (V_{GS}) due to more band bending.

3.3. Comparative study for dual work functionality: Figs. 5*a* and *b* illustrates the comparison of energy band diagram and transfer characteristics between various possible combinations of workfunction for auxiliary and tunnel gate, to maintain the dual work functionality of the device and its comparison have been shown with conventional TFET. Maintaining dual work functionality of the device, we have considered three possible combinations such as DMG TFET1 ($\phi_2 = \phi_3 > \phi_1$), DMG TFET2 ($\phi_1 = \phi_2 > \phi_3$), and DMCG-TFET ($\phi_1 = \phi_3 < \phi_2$). From the above

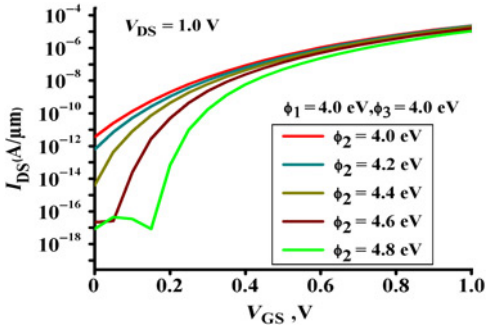


Fig. 3 *Transfer characteristics of DMCG-TFET at different control gate workfunction*

Table 2 Impact of ϕ_2 on I_{ON}, I_{OFF} and I_{ON}/I_{OFF}

ϕ_2, eV	I_{OFF}, A/μm	I_{ON}, A/μm	I_{ON}/I_{OFF}
4.0	4.27×10^{-12}	2.38×10^{-5}	5.57×10^{6}
4.2	7.65×10^{-13}	2.27×10^{-5}	2.97×10^{7}
4.4	7.01×10^{-15}	2.03×10^{-5}	2.90×10^{9}
4.6	2.29×10^{-17}	1.66×10^{-5}	7.22×10^{11}
4.8	2.57×10^{-17}	1.13×10^{-5}	4.40×10^{11}

© The Institution of Engineering and Technology 2016

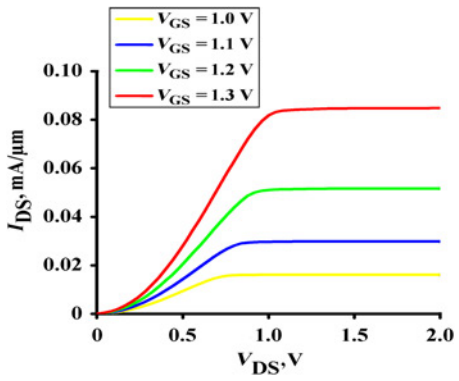


Fig. 4 *Output characteristics of DMCG-TFET at different gate to source voltage*

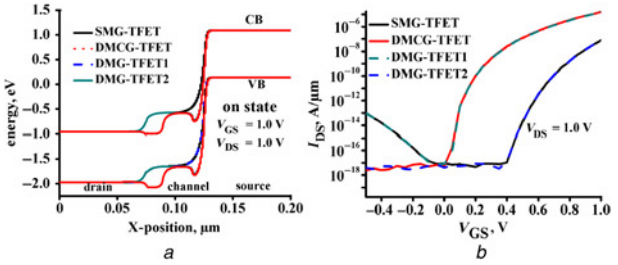


Fig. 5 *Comparison of energy band diagram and drain current for SMG-TFET, DMCG-TFET, DMG-TFET1 and DMG-TFET2*

mentioned configuration for dual workfunction, it can be observed that, by the presence of lower workfunction for the tunnel gate in case of DMCG-TFET and DMG-TFET1, reduces the depletion width at source/channel interface leads to more band bending and lower tunnelling barrier width, resulting in high ON-state current (I_{ON}). While in case of SMG TFET ($\phi_1 = \phi_2 = \phi_3$) and DMG-TFET2 have lower ON-state current (I_{ON}) in comparison with other two combinations (DMCG-TFET and DMG-TFET1) due to wider tunnelling barrier width at the source/channel interface. Further, it can be observed that among DMCG-TFET, DMG-TFET1, DMG-TFET2 and SMG-TFET, the DMCG-TFET and DMG-TFET2 suppresses the ambipolar behaviour for negative gate to source voltage (V_{GS}) as compared with other structures for asymmetric doping of source and drain regions, due to presence of lower workfunction at the auxiliary gate (ϕ_3) which widens the depletion width as shown in Fig. 6, and thus leads to suppression of ambipolar behaviour. However, in case of DMG TFET2, ON-state current (I_{ON}) is relatively far lower as shown in Fig. 5*b*. Finally, DMCG-TFET in comparison with

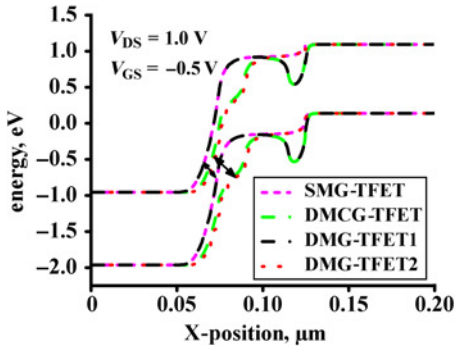


Fig. 6 *Energy band at $V_{GS} = -0.5\,V$ and $V_{DS} = 1.0\,V$ for SMG-TFET, DMCG-TFET, DMG-TFET1 and DMG-TFET2*

other structures, have been analysed to generate optimum results in terms of suppressed ambipolar behaviour and enhanced ON-state current (I_{ON}).

3.4. Effect of dielectric material and temperature variation on DMCG-TFET: A higher ON-state current (I_{ON}) and a decreased subthreshold swing (SS) can be obtained by careful selection of gate dielectric material. In this regard Fig. 7*a*, shows the effect of different dielectric material on $I_{DS} - V_{GS}$ curve of proposed device DMCG-TFET. From the same figure, we can note that ON-state current (I_{ON}) increases with the increment in value of gate dielectric permittivity, this happens due to better coupling between the gate and the tunnelling barrier. Thus, the improvement in current is exponential in nature rather than linear, hence, the improvement in SS is due to steeper part of the curve. However, the effect of temperature on the device performance can be analysed from Fig. 7*b*. In OFF-state and ambipolar condition, the trap assistant tunnelling and SRH are more dominant in comparison with BTBT. The trap assistant tunnelling and SRH are exponentially depend on temperature. Hence, leakage current and ambipolar current increase rapidly with temperature as shown Fig. 7*b*. Since, ON current depend on band to band tunnelling phenomena. BTBT is indirectly depend on temperature, thus, ON-state current (I_{ON}) slightly changes with temperature in Fig. 7*b*.

3.5. High frequency performance: The device DMCG-TFET and DMG TFET2 suppresses the ambipolar behaviour as compared with DMG TFET1 and SMG TFET, therefore, this section demonstrates the comparative analysis of high frequency performance of both the devices. For this, analogue/RF figures of merits are observed in terms of transconductance (g_m), cutoff frequency (f_T), gain band width products (GBP) and transit time τ. Theses parameters are extracted by applying a small signal 1 MHz frequency at the input port. Among these parameters, g_m play an important role for achieving higher f_T, GBP and lesser τ.

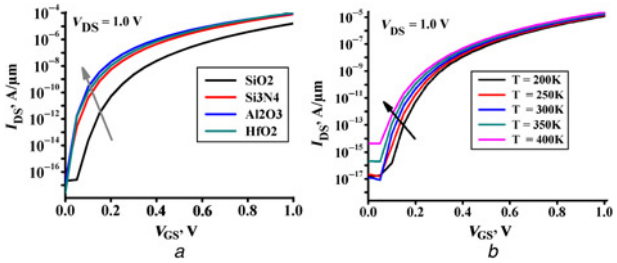


Fig. 7 *Transfer characteristics of the proposed device for*
a different dielectric materials
b different temperatures

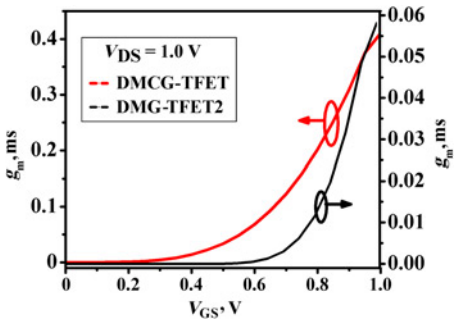


Fig. 8 *Variation of transconductance (g_m) with respect to gate to source voltage*

© The Institution of Engineering and Technology 2016

doi: 10.1049/mnl.2016.0178

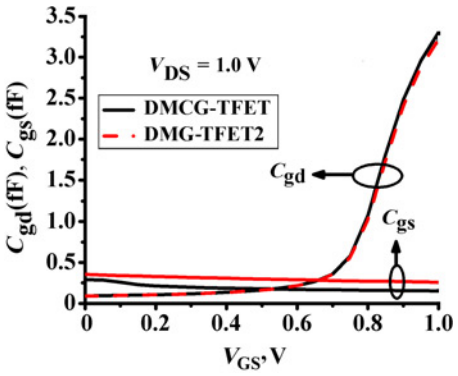


Fig. 9 *Variation of C_{gs} and C_{gd} with gate to source voltage*

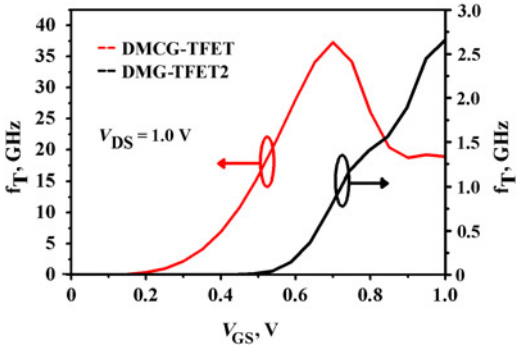


Fig. 10 *Cutoff frequency (f_T) variation as a function of gate to source voltage*

The parameter g_m can be defined as change in the drain current when unit change in gate to source voltage takes place. It decides the gain of the device and plays a major role in the design of analogue circuits. Its optimum bias point should be high enough to achieve better high frequency performance. Fig. 8 illustrates the variation of g_m with gate to source voltage for optimised device DMCG-TFET and DMG TFET2. From the figure, it can be observed that as the gate to source voltage increases the tunnelling current also increases which results in increment in g_m of both the devices, however, it decreases for higher gate to source voltage due to degradation of mobility. Further, it can be noted that g_m of DMCG TFET is greater than DMG TFET2 by the presence of lower workfunction of tunnelling gate which accumulates the electron concentration and enhances the band banding, hence, results in higher tunnel current.

The other important parameter for high frequency performance analysis is cut-off frequency. The cutoff frequency is the frequency

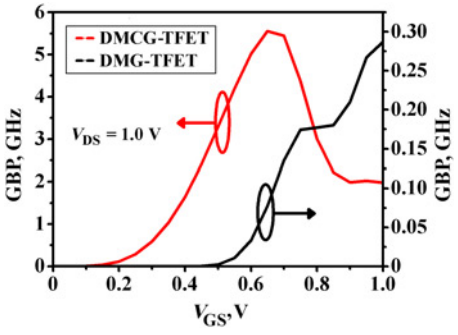


Fig. 11 *GBP variation with gate to source voltage for DMCG TFET and DMG TFET2*

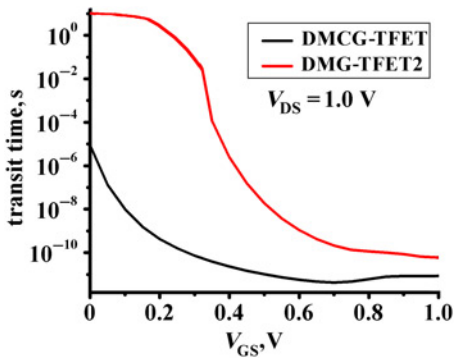


Fig. 12 *Transit time variation with gate to source voltage for DMCG TFET and DMG TFET2*

at which the short circuit current gain of the device falls to unity and is given by $f_T = g_m/2\pi(C_{gs} + C_{gd})$. It is basically depend on the ratio of g_m, gate to source capacitance (C_{gs}) and gate to drain capacitances (C_{gd}). Fig. 9 shows the variation in C_{gs} and C_{gd} with respect to V_{GS}. In case of Fig. 9*a*, C_{gd} increases with V_{GS}, due to reduction in channel to drain barrier. It also provides the better coupling between the gate and drain terminal. However, the opposite behaviour is observed in Fig. 9 for variation of C_{gs} with V_{gs}. Fig. 10 depict the initial growth of f_T with V_{GS} due to injection of charge carrier which increases the parameter g_m, and it falls for higher V_{GS} due to combined effect of accelerated increment in C_{gd} and due to mobility degradation. From the same figure, it can be analysed that the higher value of f_T is obtain for DMCG TFET as compared with DMG TFET2 due to reduced value of total capacitance and huge improvement in g_m.

The parameter GBP for DC gain 10 is obtained by GBW = $g_m/2\pi 10C_{gd}$. In Fig. 11 significant improvement in GBP for DMCG TFET and changes occurs with V_{GS} due to same reason as discussed for f_T. Fig. 12 shows the variation of transit time with V_{GS}. It is a time taken by the carrier to reach from the source region to the drain region. As the cutoff frequency increases the transit time decreases. The minimum value of τ is obtained for DMCG TFET.

4. Conclusion: In this Letter, we propose a unique design DMCG-TFET for a DMCG-TFET for asymmetric doping of the source and drain region. For this, maintaining the dual work functionality, different possible combinations of workfunctions at auxiliary gate (ϕ_3) and tunnel gate (ϕ_1) are considered. The presence of lower workfunction at auxiliary gate and tunnel gate suppresses the ambipolar behaviour and improves ON-state current (I_{ON}). The proposed device offers SS 19 mV/decade and I_{ON}/I_{OFF} ratio is $7.22 \times \sim 10^{11}$ at $V_{DS} = 1.0$ V. Apart from this, the dielectric material permittivity and temperature are important parameters which influence I_{ON} and I_{OFF} respectively of the proposed device. In this regard, the use of high-k dielectric material increases the ON-state current of the device, whereas, very minute change occurs in OFF-state current. However, the significant depredation in OFF-state current is analysed with increasing the temperature, while in ON-state current small change is observed. Finally, the significant improvement in analogue/RF performance is observed in case of DMCG TFET due to the presence of low workfunction of tunnelling gate at the source side.

5 References

[1] Seabaugh A.C., Zhang Q.: 'Low-voltage tunnel transistors for beyond CMOS logic'. Proc. IEEE, December 2010, vol. 98, no. 12, pp. 2095–2110

[2] Choi W.Y., Park B.G., Lee J.D., *ET AL.*: 'Tunneling field-effect transistors (TFETs) with subthreshold swing (SS) less than 60 mV/dec', *IEEE Electron Device Letts.*, 2007, **28**, (8), pp. 743–745

© The Institution of Engineering and Technology 2016

[3] Wang P.F., Hilsenbeck K., Nirschl T., *ET AL.*: 'Complementary tunneling transistor for low power application', *Solid-State Electron.*, 2004, **48**, (12), pp. 2281–2286
[4] Ionescu A.M., Riel H.: 'Tunnel field-effect transistors as energy efficient electronic switches', *Nature*, 2011, **479**, (7373), pp. 329–337
[5] Ionescu A.M., Michielis L.D., Dagtekin N., *ET AL.*: 'Ultra low power emerging devices and their benefits for integrated circuits'. Proc. IEEE IEDM, December 2011, pp. 16.1.1–16.1.4
[6] The international technology roadmap for semiconductors. Available at http://www.itrs.net
[7] Saurabh S., Kumar M.J.: 'Impact of strain on drain current and threshold voltage of nanoscale double gate tunnel field effect transistor (TFET): theoretical investigation and analysis', *Jpn J. Appl. Phys.*, 2009, **48**, pp. 064503
[8] Nayfeh O., Chleirigh C., Hennessy J., *ET AL.*: 'Design of tunneling field-effect transistors using strained silicon/ strained germanium type-II staggered heterojunctions', *IEEE Electron Devices Lett.*, 2008, **29**, (9), pp. 1074–1077
[9] Mohata D., Mookerjea S., Agrawal A., *ET AL.*: 'Experimental staggeredsource and N+ pocket-doped channel III-V tunnel field-effect transistors and their scalabilities', *Appl. Phys. Express 4*, 2011, **4**, pp. 024105-1–024104-3
[10] Cao W., Yao C.J., Jiao G.F., *ET AL.*: 'Improvement in reliability of tunneling field-effect transistor with p-n-i-n structure', *IEEE Trans. Electron Dev.*, 2011, **58**, (7), pp. 2122–2126
[11] Jhaveri R., Nagavarapu N.V., Woo J.C.S.: 'Effect of pocket doping and annealing schemes on the source-pocket tunnel field-effect transistor', *IEEE Trans. Electron Devices*, 2011, **58**, (1), pp. 80–86
[12] Chang H., Adams B., Chien P., *ET AL.*: 'Improved subthreshold and output characteristics of source-pocket Si tunnel FET by the application of laser annealing', *IEEE Trans. Electron Device*, 2013, **60**, (1), pp. 92–96
[13] Cui N., Liang R., Xua J.: 'Heteromaterial gate tunnel field effect transistor with lateral energy band profile modulation', *Appl. Phys. Lett.*, 2011, **98**, (142105), pp. 142105-1–142105-3
[14] Lee G., Jang J.S., Choi W.Y.: 'Dual-dielectric-constant spacer hetero-gate-dielectric tunneling field-effect transistors', *Semicond. Sci. Technol.*, 2013, **28**, (5), pp. 052001–052005
[15] Lee M.J., Choi W.Y.: 'Effects of device geometry on hetero-gate-dielectric tunneling field-effect transistors', *IEEE Electron Device Lett.*, 2012, **33**, (10), pp. 1459–1461
[16] Hraziia A., Andrei C., Vladimirescu A., *ET AL.*: 'An analysis on the ambipolar current in Si double-gate tunnel FETs', *Solid-State Electron.*, 2012, **70**, pp. 67–72
[17] Verhulst A.S., Vandenberghe W.G., Maex K., *ET AL.*: 'Tunnel field-effect transistor without gate drain overlap', *Appl. Phys.Lett.*, 2007, **91**, (5), pp. 053102–053103
[18] Lin R., Lu Q., Ranade P., *ET AL.*: 'An adjustable workfunction technology using Mo gate for CMOS devices', *IEEE Electron Device Lett.*, 2002, **23**, (1), pp. 49–51
[19] Kumar M., Haldar S., Gupta M., *ET AL.*: 'Impcat of gate material engineering (GME) on analog/RF performance of nanowire schottky barrier gate all around (GAA) MOSFET for low power wireless applications: 3D T-CAD simulation', *Microelectron. J.*, 2014, **45**, (11), pp. 1508–1514

© The Institution of Engineering and Technology 2016

doi: 10.1049/mnl.2016.0178